

# The 2.31 Ga mafic dykes in the Karelian Craton, eastern Fennoscandian shield: U–Pb age, source characteristics and implications for continental break-up processes

Alexandra V. Stepanova<sup>a,\*</sup>, Ekaterina B. Salnikova<sup>b</sup>, Alexander V. Samsonov<sup>c</sup>, Svetlana V. Egorova<sup>a</sup>, Yulia O. Larionova<sup>c</sup>, Vladimir S. Stepanov<sup>a</sup>

<sup>a</sup> Institute of Geology, Karelian Research Centre RAS, Pushkinskaya 11, Petrozavodsk, Karelia 185910, Russia

<sup>b</sup> Institute of Precambrian Geology and Geochronology RAS, Makarova 2, St. Petersburg 199034, Russia

<sup>c</sup> Institute of Geology of Ore Deposits, Petrography, Mineralogy, and Geochemistry RAS, Staromonetny 35, Moscow 119017, Russia

## ARTICLE INFO

### Article history:

Received 1 March 2014

Received in revised form

28 September 2014

Accepted 1 October 2014

Available online 23 October 2014

### Keywords:

Mafic dyke swarm

Karelian Craton

Paleoproterozoic

Supercontinent

U–Pb baddeleyite

## ABSTRACT

Major- and trace-element geochemistry, Sm–Nd isotopic and U–Pb geochronological (ID TIMS, baddeleyite) data are presented for Paleoproterozoic mafic dykes in the Karelian Craton, eastern Fennoscandian shield. Mafic dyke swarms recognized in the Lake Upper Kuito area in the Western Karelian terrane of the Karelian Craton include (i) NE-trending ca. 2450 Ma gabbronorite dykes, (ii) NW-trending ca. 2310 Ma dolerite dykes, and (iii) NNW-trending ca. 2130 Ma continental MORB-type tholeiitic dykes. Each swarm belongs to a distinct intraplate igneous event and indicates specific mantle melting and extensional processes.

The ca. 2.31 Ga doleritic dykes have high-Fe, high-Ti tholeiitic series affinity and characterized by high concentrations of lithophile trace elements. The enrichment of LREE and unfractionated HREE patterns together with depletion of Nb on multi-element diagrams and initial  $\epsilon_{\text{Nd}}$  values of +0.5 to +0.8 are characteristic for ca. 2.31 Ga dolerites. The geochemical modelling results suggest that these features could be originated via combination of fractional crystallization and crustal contamination processes, and do not indicative of a mantle source enrichment. It also indicates long-term storage of melts in an intracrustal magma chamber and a relatively slow ascent to the surface. The primary melts of ca. 2.31 Ga dolerites possibly originated by partial melting of a DM-type mantle source in the spinel peridotite stability field.

In contrast to previous ca. 2.45 Ga event studied ca. 2.31 Ga dolerites do not indicate high-temperature mantle-plume induced mantle melting. On the other hand, the ca. 2.31 Ga dykes have some similarities with syn-breakup ca. 2.13 Ga continental MORB-type tholeiites, although there is no evidence for the break-up of the continental lithosphere of the Karelian Craton at ca. 2.31 Ga. Thus ca. 2.31 Ga dykes could indicate the existence of relatively stable extensional tectonic environment and an unsuccessful attempt of break-up of the continent.

The ca. 2.31 Ga dykes together with previously studied Runkaus basalts and Taivalkoski dykes could be considered as a component of distinct relatively wide-spread Kuito-Taivalkoski igneous event within the ca. 2.2–2.4 Ga “crustal age gap” period in the eastern Fennoscandian shield. This probably indicate that the number and intensity of endogenous events of age 2.4–2.2 Ga are greatly undervalued. This also argues against a decrease of endogenic activity and magmatic “slowdown” during ca. 2.4–2.2 Ga period.

© 2014 Elsevier B.V. All rights reserved.

## 1. Introduction

Mafic dykes are useful instrument in recognizing mantle and crustal events in the Earth history because they could give reliable

information on age of igneous events, mantle melting processes, crustal tectonics and sometimes these data allow us to recognize a mantle plume ascent and/or continents break-up.

In the Paleoproterozoic, several global igneous events (ca. 2.5–2.4, 2.2, 2.1, 2.0–1.98 Ga, etc.) have been recognized by studying mafic dykes in different Precambrian shields (Ernst and Buchan, 2001; Bleeker and Ernst, 2006). These are also important as the plumbing system of large igneous provinces (LIPs) (Ernst, 2014).

\* Corresponding author. Tel.: +78142782753; fax: +78142760602.  
E-mail address: [stepanov@krc.karelia.ru](mailto:stepanov@krc.karelia.ru) (A.V. Stepanova).



The early Paleoproterozoic ca. 2.5–2.4 Ga event is characterized by a wide distribution of high-Mg mafic dykes, volcanic rocks and layered intrusions indicative of a high-temperature, deep-seated mantle melting event related to the ascent of a mantle plume (Puchtel et al., 1997; Vogel et al., 1998; Bleeker and Ernst, 2006; Bayanova et al., 2009) and in comparison with the formerly adjacent Superior craton divide into two distinct LIP/plume events, as c. 2500 and 2450 Ma (Kulikov et al., 2010). The next ca. 2.2 Ga global-scale event includes mafic dykes and sills that occur in several Precambrian shields (Maurice et al., 2009; French and Heaman, 2010; Hanski et al., 2010). This event is not as homogenous as the mentioned above ca. 2.45–2.5 Ga one but also indicates widespread mantle melting processes probably caused by mantle plume activity. A lot of information is also available on the ca. 2.1, 2.0, and 1.98 Ga magmatic events (Puchtel et al., 1998; Hanski et al., 2001a; Aspler et al., 2002; Modeland et al., 2003; Bleeker and Ernst, 2006; Vuollo and Huhma, 2005; Stepanova et al., 2014a).

In contrast, information on igneous events that took place within the time interval of ca. 2.4–2.2 Ga is more restricted (Condie et al., 2009; Ernst and Bleeker, 2010). The apparent global scarcity of the ca. 2.4–2.2 Ga igneous rocks has led to a suggestion that this time represents a “crustal age gap” or “magmatic slowdown” period dominated by continental sedimentary processes (Condie et al., 2009; Eriksson and Condie, 2014). However, recent investigations indicate that igneous events including intrusion of granitoids and mafic dyke swarms with an age between 2.4 and 2.2 Ga occur in different Precambrian shields (Kusky and Li, 2003; French and Heaman, 2010; Nilsson et al., 2012; Partin et al., 2014; Salminen et al., 2014).

In the Karelian Craton, mafic rocks with an age ca. 2.3 Ga have been recognized previously. They include the Runkaus Formation volcanic rocks in the Peräpohja schist belt (Huhma et al., 1990) and sporadic mafic dykes in the Archaean basement (Vuollo and Huhma, 2005; Salminen et al., 2014), but their geochemical features, isotopic characteristics and tectonic position have not previously been discussed in detail. In this contribution, new U–Pb age determinations and geochemical and Sm–Nd isotopic data are reported for a ca. 2.3 Ga mafic dyke swarm in Russian Karelia and the petrological and tectonic processes responsible for the origin of these dykes are evaluated. Also the newly recognized event is compared with previous and subsequent episodes of intraplate magmatic activity in the Karelian Craton.

## 2. Geological background

The Karelian Craton is a large Archaean composite granite-greenstone terrane in the eastern part of the Fennoscandian Shield bounded in the SW and NE by the Svecofennian and Lapland-Kola Paleoproterozoic orogens, respectively (Fig. 1). The craton is subdivided into the Western Karelian, Central Karelian, and Vodlozero terranes with different ages of crust formation (Lobach-Zhuchenko et al., 2000). The Vodlozero and Western Karelian terranes comprise Paleoarchaean (3.5–3.2 Ga) tonalite–trondhjemite–granodiorite (TTG) gneiss cores surrounded by Meso- and Neoproterozoic tonalite–greenstone belts. These terranes are separated by juvenile Neoproterozoic (2.74–2.69 Ga) complexes of the Central Karelian terrane, which is dominated by sanukitoid series batholiths with relicts of tonalite–greenstone belts (Kovalenko et al., 2005; Heilimo et al., 2011).

The Paleoproterozoic history of the Karelian Craton includes accumulation of different types of marine and continental sediments and several pulses of within-plate magmatism (Hanski, 2013; Melezhik and Hanski, 2013 and references therein) thought to belong to large igneous province (LIP) events. Mafic dykes, volcanic rocks, sills, and layered intrusions with ages of ca.

2.51–2.45 Ga and ca. 2.06–1.95 Ga are widespread and well-studied in the Karelian Craton (Puchtel et al., 1997, 1998; Sharkov and Smolkin, 1997; Vogel et al., 1998; Hanski et al., 2001a,b; Iljina and Hanski, 2005; Vuollo and Huhma, 2005).

The ca. 2.50–2.45 Ga event is characterized by the presence of komatiitic, basaltic, and felsic volcanic rocks and siliciclastic sediments formed in rift-related volcano-sedimentary belts synchronous with layered mafic intrusions, granite massifs, and gabbro-dyke swarms (Buiko et al., 1995; Puchtel et al., 1997; Vuollo and Huhma, 2005; Kulikov et al., 2010; Korsakova et al., 2011; Lauri et al., 2012). It is generally assumed that mantle and crust melting at ca. 2.50–2.45 Ga was caused by the ascent of a mantle plume that produced a LIP that affected an extensive area in the Karelian and Superior cratons which were attached at this time (Puchtel et al., 1997; Vogel et al., 1998; Bleeker and Ernst, 2006; Kulikov et al., 2010). The younger Sarioian (2.4–2.3 Ga) mafic volcanic rocks that are relatively widespread in Finland and Kola Peninsula vary in composition from komatiites to andesites and have geochemical and isotopic characteristics close to those of ca. 2.45 Ga high-Mg rocks in the Russian part of the Karelian Craton (Räsänen et al., 1989; Puchtel et al., 1997; Hanski, 2013).

The ca. 2.06–1.95 Ga events comprise diverse, plume-related mafic complexes that include picrites, high- and low-Ti tholeiites, subalkaline basalts, syenites, carbonatites, and kimberlites (Puchtel et al., 1998; Philippov et al., 2007; Corfu et al., 2011; Glushanin et al., 2011; Vuollo and Huhma, 2005). These magmatic complexes were accompanied by terrigenous sedimentary sequences, containing black shales, accumulated in the Omega and Salla-Kuolajärvi Basins (Glushanin et al., 2011; Hanski and Melezhik, 2013).

In contrast to the plume-related events discussed above, the ca. 2.3–2.06 Ga period (Jatuli in the regional stratigraphy) is presented by volcano-sedimentary sequences of relatively homogeneous intraplate tholeiitic series basalts and sills interbedded with marine and continental sediments (Glushanin et al., 2011; Hanski and Melezhik, 2013). The compositional homogeneity of basalts was perhaps the reason for the consideration of all ca. 2.3–2.06 Ga mafic igneous rocks in the frame of single continental flood basalt (trap) event (Svetov, 1979; Malashin et al., 2003). However, precise geochronological studies indicate that this magmatism could be subdivided into a number of discrete magmatic events: Jatulian igneous rocks have defined an age of ca. 2.22 Ga for the mafic sills of the gabbro-wehrlite association (Hanski et al., 2010) and ca. 2.1 Ga for the Fe-tholeiitic (Nykänen et al., 1994; Vuollo and Huhma, 2005) and continental MORB-type tholeiitic (Stepanova et al., 2014b) mafic dyke swarms in the Karelian Craton. These are also linked to corresponding LIP events in the formerly adjacent Superior craton (Bleeker and Ernst, 2006; Ernst and Bleeker, 2010). Recently, Salminen et al. (2014) reported new geochronological and paleomagnetic data for doleritic dykes showing an age of ca. 2.34 Ga. This together with our results argues for the existence of a distinct intraplate igneous event at ca. 2.3 Ga in the Karelian Craton. We have studied mafic dykes occurring in the Lake Upper Kuito area in the eastern part of the Western Karelian terrane where a large number of Paleoproterozoic mafic dykes were recognized previously (Ein, 1984) in the Archaean rocks of the Voinytsa and Voknavolok domains (Fig. 1).

The Voknavolok domain is mostly composed late-tectonic orthopyroxene-bearing granitoids with amphibolite inclusions, belonging the Voknavolok granulite complex that preserve relicts of granulite facies mineral assemblages (Kozhevnikov, 1982) formed at a relatively low P of 1.8–4.1 kbar and a high T of  $677 \pm 36$  °C (Samsonov et al., 2001). The late-tectonic granitoids are adakite-series, high-Al trondhjemites strongly depleted in U and Th. The U–Pb zircon age of  $2745 \pm 4$  Ma obtained by Bibikova et al. (2005) defines the crystallization age of trondhjemites. The



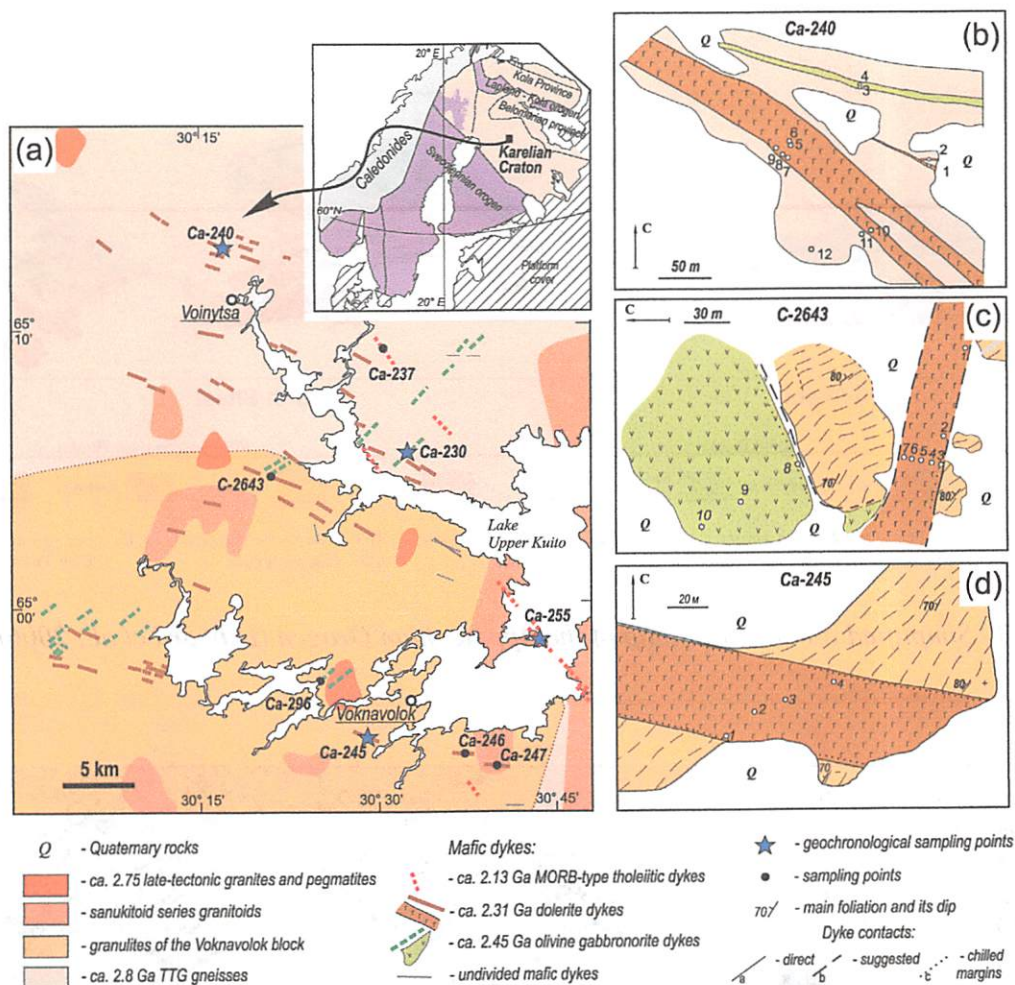


Fig. 1. Schematic geological map of the Voinytsa-Voknavolok area (after 1: 2,000,000 Geological Map of the Baltic Shield (1999), Ein (1984), Bibikova et al. (2005), Samsonov et al. (2001)) with the main tectonic structures of the Fennoscandian Shield shown in the insert (after Hölttä et al., 2008); (b) schematic map of sampling site Ca-240; (c) schematic map of sampling site C-2643 showing cross-cutting of gabbro-norite and dolerite dykes; (d) schematic map of sampling site Ca-245.

initial  $\epsilon_{Nd}$  values of +1.4 (Lobach-Zhuchenko et al., 2000) indicates a short crustal residence time for the source of trondhjemites.

The TTG gneisses with intrusive protolith of age  $2788 \pm 12$  Ma predominate among the Archaean crustal rocks in the Voinytsa domain. They are cross-cut by small intrusions of the late- and post-tectonic sanukitoid series granitoids with an age of  $2714 \pm 9$  Ma (U–Pb zircon data; Bibikova et al., 2005). Both TTG gneisses and sanukitoid series granitoids are analogues to the well-studied gneisses and granitoids of the Kostomuksha domain where TTG magmas have a juvenile mafic source ( $\epsilon_{Nd(2.8\text{ Ga})} = +1.9$ ) while the sanukitoid series rocks indicate contribution from an ancient crustal component ( $\epsilon_{Nd(2.72\text{ Ga})}$  varies from +1.92 to –0.62) (Samsonov et al., 2004; Larionova et al., 2007).

The Western Karelian terrane was thermally overprinted during the 1.9–1.8 Ga Svecofennian orogeny, but at very low degree (Kontinen et al., 1982). The latest metamorphic overprinting is localized in narrow shear zones with an age ca. 1.72 Ga (Larionova et al., 2013).

### 3. Sampling and analytical techniques

The sampling sites are shown on the map of Fig. 1. Each swarm was sampled at several locations along its strike (NE and NNW swarms) or across it (NW swarm) (Fig. 1). Samples from individual dykes were collected from the chilled margin zones and medium- to

coarse-grained dykes central parts. The sampled dykes were studied using a combination of petrographic, geochemical, and isotopic methods.

Baddeleyite from medium-grained dolerite samples was extracted using a Wilfley shaking table at the Institute of Geology of Ore deposits, Geochemistry, Mineralogy and Petrography, Russian Academy of Sciences (IGEM RAS), Moscow, following the method described by Söderlund and Johansson (2002). Up to 200 baddeleyite grains with a size range of 20–80  $\mu\text{m}$  were extracted from each sample of weight up to 2.0 kg.

Concentrations of major elements were determined on fused glass discs using a PW-2400 X-ray sequential fluorescence spectrometer at IGEM RAS. The uncertainties were 1–5% for elements with concentrations of >0.5 wt.% and up to 12% for elements with concentrations of <0.5 wt.%. Loss on ignition (LOI) values were determined gravimetrically.

The concentrations of lithophile trace elements were determined by inductively coupled plasma mass-spectrometry (ICP-MS) using an XSeries 2 instrument at the Institute of Geology Karelian Research Centre RAS (IG KarRC RAS), Pertozaodsk. Powdered samples were digested in acid mixture following the standard procedure described by Karandashev et al. (2008). The accuracy of the analyses was monitored by analyzing the USGS standards BHVO2, GSP-2, and BIR-1a, and in-house reference materials. The accuracy for most trace elements was ca. 7%, with the exception of



Nb (10–15%) and Pb (up to 15%). The uncertainties in the concentrations of Be, Zr, Hf, and Ta were 25–40% due to poor analytical reproducibility; ICP-MS data for these elements are not reported here. The reported concentrations of Zr were analyzed by XRF using a PW-2400 spectrometer at IGEM RAS. The accuracy of XRF analyses for Zr monitored using the BHVO2, BIR-1a and in-house reference materials was better than 10%. Compositions of minerals were determined at the IG KarRC RAS using a Tescan Vega II LSH electron microprobe with EDS INCA-Energy 350. Operating conditions were 20 kV accelerating voltage, 15 nA beam current, and 10  $\mu\text{m}$  beam size.

The U–Pb baddeleyite study was carried out in the Laboratory of Isotope Geology, Institute of Precambrian Geology and Geochronology (IPGG RAS), Saint-Petersburg employing the isotope dilution thermal ionization mass-spectrometry technique (ID-TIMS). Hand-picked, most transparent and homogeneous baddeleyite grains were ultrasonically washed in ethanol and acetone. To eliminate surface contamination, additional soft acid washing was performed using warm 1 M  $\text{HNO}_3$  and 1 M HCl for 20 min each. Then grains (9–30 per analysis) were transferred to the Teflon digestion vessel in a high-pressure, stainless steel-jacketed Teflon bomb (Parr bombs) and spiked with a  $^{202}\text{Pb}$ – $^{235}\text{U}$  isotopic solution. The grains were dissolved in 10  $\mu\text{l}$  HF at 220 °C overnight. No column chemistry was performed. Isotopic analyses were carried out on a Triton TI multicollector mass spectrometer in ion counting mode.

The uncertainties on the U/Pb ratio were 0.5%, and the blanks were 1–5 pg for Pb and 1 pg for U. The data were reduced using the PbDAT (Ludwig, 1989) and ISOPLOT (Ludwig, 2003) software. The common Pb correction was applied according to the model of Stacey and Kramers (1975). All errors are reported as  $2\sigma_{\text{mean}}$ .

The Sm–Nd isotopic data were obtained at the Laboratory of Isotope Geochemistry and Geochronology, IGEM RAS following the analytical protocol described in Stepanova et al. (2014b).

## 4. Results

During Paleoproterozoic LIP/rifting events over the interval ca. 2.45–1.97 Ga, numerous mafic dykes were emplaced into the Archaean crust of the Western Karelia terrane (Ein, 1984; Vuollo and Huhma, 2005). In the Lake Upper Kuito area they form several swarms with a NW, NNW, or NE direction (Ein, 1984) (Fig. 1a). Below we give a short description of the previously-studied ca. 2.13 Ga NNE swarm, new compositional and age data for the ca. 2.45 Ga, NE-trending swarm and a detailed description of the ca. 2.31 Ga, NW-trending swarm that is the main object of this study.

### 4.1. The 2.13 Ga Pirtguba swarm

The ca. 2.13 Ga mafic dykes form a narrow (ca. 10 km), NNW-trending swarm that can be traced for more than 30 km. The dykes within this swarm are up to 50 m thick and have a strike length of several kilometres (Fig. 1). Most of the dykes are well-preserved. The detailed description of the Pirtguba (Ca-255) and Allajarvi (Ca-237) localities (Fig. 1a) has been documented by Stepanova et al. (2014b).

The ca. 2.13 Ga dykes are composed of olivine-bearing dolerites. The dyke margins usually comprise fine-grained clinopyroxene-plagioclase dolerite with rare plagioclase and olivine phenocrysts. The central parts of the studied ca. 2.13 Ga dykes usually consist of medium-grained olivine-bearing dolerite and gabbro with small gabbro-pegmatite schlieren. The main minerals of the dolerites are plagioclase ( $X_{\text{Mg}} = 0.80$ – $0.68$ ), low-Ca pyroxene ( $X_{\text{Mg}} = 0.78$ – $0.48$ ), and olivine ( $\text{Fo}_{48-50}$ ). Amphibole (Fe-edenite) forms an essential part of the late-magmatic mineral

assemblage. The dykes also contain a lot of baddeleyite and zircon, with both of them being well-preserved. Zircon grains from the Pirtguba locality were dated using the SHRIMP-II instrument and gave a U–Pb age of  $2126 \pm 5$  Ma that is interpreted to be the emplacement age of the dyke (Stepanova et al., 2014b).

The ca. 2.13 Ga dykes have a continental MORB-type tholeiitic affinity. The MgO contents range between 7.44 wt.% in the chilled margin zones and 4.14 wt.% in gabbro-pegmatite,  $\text{TiO}_2$  – between 1.06 and 1.27 wt.% (Figs. 3 and 4). These dykes have relatively high  $\text{Fe}_2\text{O}_3^{\text{tot}}$  and V, and low Cr, Ni, and Co concentrations, and low contents of HFSE and REE (Stepanova et al., 2014b). They are characterized by essentially unfractionated chondrite-normalized LREE ( $(\text{La}/\text{Sm})_n = 0.9$ – $1.2$ ) and HREE ( $(\text{Gd}/\text{Yb})_n = 1.0$ – $1.2$ ) patterns and small positive Ti, Nb, and Zr anomalies on the primitive mantle-normalized diagrams (Fig. 5). Studied whole-rock samples of ca. 2.13 Ga continental MORB-type tholeiites in the Lake Upper Kuito area (site Ca-255) have positive initial  $\epsilon_{\text{Nd}}$  values ranging from +1.4 in the chilled margin zone to +2.8 in the central part of the dyke (Stepanova et al., 2014b).

### 4.2. The 2.45 Ga Lashkujarvi swarm

In the studied area, the NE-trending dykes form a narrow swarm that can be traced for ca. 30 km along its strike (Fig. 1). The swarm consists of gabbro-diorite dykes that vary in thickness from 10 m up to several hundreds of metres. The dykes were studied previously by Ein (1984), and based on their mineral and chemical composition, the dykes are considered to belong to the ca. 2.45 Ga age group. The NE-trending dykes of similar composition and age were described by Vuollo and Huhma (2005) as boninite-norite dykes.

Many of the dykes in this swarm have been altered under greenschist facies conditions. They usually preserve relicts of plagioclase grains but pyroxenes and olivine are completely altered and replaced by fibrous amphibole. The chilled fine-grained, pyroxenophytic rocks along the contacts, if preserved (e.g. site Ca-296, Fig. 1), are composed of orthopyroxene, clinopyroxene and plagioclase. The central parts of several dykes are well-preserved and consist of medium- and coarse-grained olivine gabbro-diorite. These rocks still contain primary magmatic olivine, chromite, orthopyroxene, clinopyroxene and plagioclase. Dark-coloured olivine ( $\text{Fo}_{75}$ ) forms up to 10% of the rock volume. Orthopyroxene ( $X_{\text{Mg}} = 0.88$ ) forms unzoned prismatic grains that are often surrounded by a hyperssthene ( $X_{\text{Mg}} = 0.80$ ) or augite ( $X_{\text{Mg}} = 0.65$ ) “rim”. Augite ( $X_{\text{Mg}} = 0.78$ ) also forms small, prismatic and anhedral grains that contain small anhedral chromite inclusions. Plagioclase in the gabbro-diorites varies in composition from  $\text{An}_{57}$  to  $\text{An}_{46}$ . Interstices between primary magmatic minerals are sometimes filled with quartz-feldspar granophyre that forms up to 1–3% of the rock volume and contains rare baddeleyite grains.

The gabbro-diorites of the NE-trending swarm are high-Mg rocks with the MgO content varying from ca. 8 wt.% in the chilled margin rocks up to 17.9 wt.% in the olivine gabbro-diorites in the central parts of the dykes. High concentrations of Cr (up to 2198 ppm), Ni (up to 1000 ppm) and low contents of  $\text{TiO}_2$  (0.47–0.84 wt.%) are characteristic for these gabbro-diorites (Fig. 4). At the same time, they are relatively high in  $\text{SiO}_2$  (up to 52 wt.%) (Fig. 3, Table 1).

The gabbro-diorites are characterized by a strong depletion of Nb on the multi-element diagrams (Fig. 5) and their  $\text{Nb}/\text{Nb}^* = [\text{Nb}_{\text{PM}}/(\text{Th}_{\text{PM}} * \text{La}_{\text{PM}})^{1/2}]$  values vary from 0.36 to 0.17. They show fractionated REE patterns with LREE enrichment and HREE depletion ( $(\text{La}/\text{Sm})_n = 2.2$ – $2.9$ ,  $(\text{Gd}/\text{Yb})_n = 1.7$ ) (Figs. 4 and 5). The studied gabbro-diorites from site Ca-230 have an initial  $\epsilon_{\text{Nd}}$  of  $-1.7$  (Table 1).

More than 100 baddeleyite grains were extracted from a medium-grained olivine gabbro-diorite (sample Ca-230-3, central

**Table 1**  
Chemical and Nd isotopic composition of dolerite and gabbrorite dykes of the Lake Upper Kuito area.

	Voimytša						Aiguba			
	Ca-240-1 Dolerite	Ca-240-2 Dolerite	Ca-240-5 Dolerite	Ca-240-7 Dolerite	Ca-240-8 Dolerite	Ca-240-10 Dolerite	C-2643-3 Dolerite	C-2643-5 Dolerite	C-2643-7 Dolerite	Ca-299-1 Dolerite
SiO <sub>2</sub>	49.85	50.04	48.83	49.51	49.36	49.32	50.92	50.47	51.36	48.21
TiO <sub>2</sub>	2.21	2.13	2.49	2.15	2.22	2.25	2.14	1.92	2.23	2.66
Al <sub>2</sub> O <sub>3</sub>	11.67	11.44	12.45	13.47	13.52	12.60	13.06	13.35	13.34	12.10
Fe <sub>2</sub> O <sub>3</sub>	19.24	19.34	19.73	18.29	18.65	19.10	17.70	17.81	17.42	18.78
MnO	0.244	0.259	0.252	0.242	0.237	0.250	0.25	0.25	0.26	0.25
MgO	3.89	4.05	3.38	3.28	2.91	3.44	5.12	4.86	5.56	3.97
CaO	9.45	8.94	9.05	9.26	9.11	9.25	8.99	9.64	8.89	9.27
Na <sub>2</sub> O	1.91	1.55	2.28	2.37	2.52	2.32	2.34	2.32	1.74	2.39
K <sub>2</sub> O	0.79	1.38	0.96	0.86	0.90	0.90	0.75	0.70	0.42	0.73
P <sub>2</sub> O <sub>5</sub>	0.24	0.19	0.25	0.27	0.25	0.23	0.24	0.21	0.25	0.30
S	0.06	0.06	0.08	0.06	0.10	0.09	<0.02	<0.02	<0.02	0.09
LOI	0.22	0.39	<0.02	<0.02	<0.02	<0.02	1.32	0.26	1.58	0.78
<i>ppm</i>										
Li	11.5	35.9	3.52	6.03	5.35	5.36	3.74	9.02	7.34	11.1
Sc	41.4	47.5	40.56	40.34	39.00	42.17	36.53	38.17	38.50	
V	439	506	502	424	427	460	405	395	416	348
Cr	66.7	82.6	64.4	60.3	58.3	64.5	151.2	84.1	86.9	37.3
Co	49.9	50.9	52.1	47.7	50.6	48.1	49.8	49.1	51.0	40.1
Ni	46.4	51.7	47.2	46.0	44.2	45.4	66.41	61.2	60.9	32.2
Cu	267	266	330	259	287	269	300	323	230	227
Rb	24.3	41.7	25.9	20.5	22.0	23.5	23.0	18.8	2.85	12.6
Sr	157	125	162	153	158	154	155	153	124	133
Y	40.57	42.44	39.55	41.47	38.81	42.48	38.47	35.81	39.33	44.1
Zr	162	164	170	155	171	160	112	89.9	52.0	151
Nb	9.98	10.2	11.9	10.3	11.0	10.5	10.7	9.65	11.1	11.1
Ba	224	294	319	272	271	268	167	169	39.2	127
La	16.4	16.7	18.3	16.5	17.8	16.4	16.1	15.5	16.1	18.4
Ce	36.1	36.1	41.9	35.8	40.8	35.9	40.8	37.5	37.9	44.2
Pr	4.72	4.76	5.44	4.71	5.32	4.68	4.19	3.80	3.85	5.89
Nd	20.5	20.8	23.4	20.6	22.9	20.6	23.6	21.4	22.1	26.9
Sm	6.12	6.22	6.40	6.23	6.25	6.25	6.25	5.65	5.78	6.71
Eu	1.88	1.87	1.98	1.91	1.91	1.92	1.97	1.83	1.88	1.89
Gd	6.40	6.50	7.24	6.63	7.16	6.46	6.44	5.79	6.11	8.78
Tb	1.04	1.07	1.11	1.07	1.12	1.07	1.31	1.18	1.25	1.34
Dy	7.39	7.91	6.60	7.53	6.47	7.58	8.29	7.59	8.08	8.51
Ho	1.55	1.57	1.49	1.59	1.50	1.58	1.70	1.55	1.68	1.73
Er	4.53	4.55	4.76	4.62	4.69	4.67	5.03	4.61	4.98	5.15
Tm	0.648	0.655	0.680	0.652	0.668	0.666	0.728	0.686	0.732	0.714
Yb	4.51	4.31	4.64	4.55	4.55	4.67	5.03	4.56	4.74	4.60
Lu	0.626	0.608	0.688	0.644	0.676	0.652	0.707	0.651	0.696	0.688
Pb	3.92	3.11	7.60	5.43	6.60	8.24	8.98	9.36	2.54	5.45
Th	3.19	3.07	3.63	3.27	3.50	3.20	3.53	3.14	2.96	3.47
U	0.443	0.414	0.540	0.436	0.516	0.436	0.585	0.491	0.489	0.518
<sup>147</sup> Sm/ <sup>144</sup> Nd			0.1513							
<sup>143</sup> Nd/ <sup>144</sup> Nd			0.511980							
<sup>ε</sup> Nd (2310)			+0.7							
<i>ppm</i>										
Voknavolok						Lashkujarvi				
	Ca-245-1 Dolerite	Ca-245-3 Dolerite	Ca-245-4 Dolerite	Ca-246-1 Dolerite	Ca-247-1 Dolerite	Ca-247-2 Dolerite	Ca-230-1 Ol gabbrorite	Ca-230-2 Ol gabbrorite	Ca-230-3 Ol gabbrorite	
SiO <sub>2</sub>	49.83	49.22	49.33	49.61	50.08	50.28	50.66	49.60	51.36	
TiO <sub>2</sub>	2.60	2.57	2.57	2.27	2.25	2.09	0.57	0.55	0.47	
Al <sub>2</sub> O <sub>3</sub>	11.34	12.93	13.25	12.16	12.66	12.16	8.45	9.04	9.11	
Fe <sub>2</sub> O <sub>3</sub>	19.83	18.75	18.62	17.72	17.91	17.58	11.09	11.34	10.73	
MnO	0.241	0.225	0.222	0.236	0.224	0.226	0.191	0.187	0.176	
MgO	3.67	3.15	2.89	4.64	3.87	4.50	16.84	17.89	17.26	
CaO	8.98	9.00	8.85	9.09	9.02	9.48	7.46	7.16	7.59	
Na <sub>2</sub> O	1.64	2.36	2.43	2.65	2.18	2.09	1.48	1.23	1.48	
K <sub>2</sub> O	1.07	1.11	1.11	0.71	1.03	0.82	0.65	0.56	0.51	
P <sub>2</sub> O <sub>5</sub>	0.31	0.36	0.37	0.25	0.30	0.23	0.07	0.07	0.06	
S	0.07	0.06	0.08	0.03	0.08	0.06	0.04	<0.02	0.04	
LOI	0.15	49.22	<0.02	0.40	0.16	0.26	1.96	1.87	0.73	
<i>ppm</i>										
Li	7.96	6.09	11.3	15.3	5.76	9.41	18.8	18.3	12.0	
Sc	40.5	41.5	40.7	43.6	39.7	39.4	20.7	22.3	22.5	
V	426	475	440	395	387	387	112	141	135	
Cr	43.2	46.7	37.6	89.3	63.4	83.0	1653	1733	1850	
Co	48.2	49.0	47.6	44.7	46.2	43.2	74.8	72.5	71.2	
Ni	38.4	41.4	37.7	55.8	48.5	49.8	660	604	584	
Cu	357	341	379	253	327	244	77.8	71.3	67.3	
Rb	31.1	30.64	30.2	19.6	26.3	23.0	25.5	17.8	18.7	



Table 1 (Continued)

	Voknavolok						Lashkujarvi		
	Ca-245-1 Dolerite	Ca-245-3 Dolerite	Ca-245-4 Dolerite	Ca-246-1 Dolerite	Ca-247-1 Dolerite	Ca-247-2 Dolerite	Ca-230-1 Ol gabbronorite	Ca-230-2 Ol gabbronorite	Ca-230-3 Ol gabbronorite
Sr	134	141.89	134	154	160	156	147	134	138
Y	51.7	50.33	51.5	41.9	44.6	40.0	9.18	9.09	7.86
Zr	225	198.06	216	176	195	177	71	68	61
Nb	13.3	13.15	13.3	11.6	12.9	11.5	2.01	2.18	1.88
Ba	314	312.08	307	210	333	262	191	152	171
La	17.6	19.97	20.9	19.5	20.9	18.0	7.77	4.70	6.59
Ce	40.5	43.02	45.1	40.4	44.6	39.1	16.5	11.4	14.2
Pr	5.34	5.66	5.89	5.28	5.76	5.05	1.93	1.45	1.68
Nd	23.3	24.72	25.6	22.6	24.8	22.0	7.79	6.04	6.71
Sm	7.33	7.53	7.71	6.55	7.20	6.40	1.99	1.93	1.73
Eu	2.04	2.11	2.15	1.87	2.06	1.85	0.59	0.61	0.54
Gd	7.68	7.78	7.87	6.56	7.19	6.44	2.04	2.00	1.73
Tb	1.30	1.28	1.30	1.08	1.16	1.05	0.30	0.29	0.26
Dy	9.35	9.08	9.29	7.49	8.09	7.38	1.34	1.35	1.14
Ho	1.95	1.90	1.92	1.56	1.70	1.53	0.36	0.36	0.31
Er	5.78	5.53	5.69	4.57	4.90	4.47	1.07	1.08	0.95
Tm	0.817	0.78	0.796	0.644	0.698	0.626	0.140	0.144	0.124
Yb	5.79	5.46	5.54	4.48	4.93	4.38	0.98	0.97	0.84
Lu	0.792	0.76	0.770	0.630	0.673	0.612	0.136	0.140	0.124
Pb	4.70	11.02	4.38	4.83	5.19	4.31	7.08	5.46	3.55
Th	4.64	4.41	4.63	3.82	4.23	3.83	2.05	1.94	1.78
U	0.803	0.71	0.770	0.461	0.569	0.500	0.400	0.36	0.36
<sup>147</sup> Sm/ <sup>144</sup> Nd		0.1522	0.1516						0.1362
<sup>143</sup> Nd/ <sup>144</sup> Nd		0.511984	0.511993						0.511572
$\epsilon_{Nd}$ (2310)		+0.5	+0.8						-1.7

part of the dyke, ca. 2.0 kg). Most of the grains are well-preserved, transparent, light-brown and long-prismatic in habit. The range in grain size is 20–40  $\mu\text{m}$ . Three fractions (10–15 grains) of dark brown, tabular baddeleyite grains were analyzed (Table 2, lines 1–3). Data points are slightly discordant, yielding an upper intercept age of  $2450 \pm 12$  Ma (MSWD=0.17) (Fig. 7), which is interpreted as the dyke emplacement age. The lower intercept is at  $1416 \pm 450$  Ma.

#### 4.3. The 2.31 Ga Kuito swarm

##### 4.3.1. Geology and mineral composition

The NW-trending (300–310°) dykes form a regular swarm, which was traced in a wide territory with a width of ca. 40 km and length of ca. 50 km (Ein, 1984) (Fig. 1a). According to the data of Vuollo and Huhma (2005) and Salminen et al. (2014), this swarm may continue to the neighbouring territory of Finland and probably forms the most wide-spread dyke generation in the studied area. The dykes vary in thickness from several metres up to 50 m (Fig. 1b–d). A cross-cutting relationships between two dykes of different orientation occur in the Aiguba area, where the NW-trending (310°) dolerite dyke cross-cuts the NE-trending olivine gabbronorite dyke that belongs to the ca. 2.45 Ga swarm (site C-2643, Fig. 1a and c).

Most of the dykes are well-preserved and can be followed along the strike for several hundreds of metres. The others are fragmented and altered under epidote amphibolite facies conditions. This alteration is probably related to late shearing tectonics that, according to the Rb–Sr and Sm–Nd data, occurred in the Karelian Craton at ca. 1.7–1.5 Ga (Amelin and Semenov, 1996; Larionova et al., 2013). Several dykes (e.g. dyke at Site Ca-240, Fig. 1a and b) have complicated morphological features, e.g., bifurcation, apophyses and xenoliths of host rocks, and show evidence for small-scale crustal remelting or absorption of crustal material at the dyke margin. Chilled margin zones of the dykes are composed of fine-grained dolerite-porphyrines with clinopyroxene and plagioclase phenocrysts (Fig. 2a). The inner parts of plagioclase laths are unzoned and composed of An<sub>51–49</sub>. The plagioclase

phenocrysts sometimes contain rare small (20–30  $\mu\text{m}$ ), anhedral inclusions of Ba-bearing potassium feldspar. The clinopyroxene phenocrysts occur as unzoned laths (Fig. 2a) and are composed of both augite and pigeonite ( $X_{\text{Mg}}=0.67–0.59$ ).

The groundmass of dolerite-porphyrines (Fig. 2a) consists of plagioclase (An<sub>43</sub>), clinopyroxene, amphibole, Fe-oxides and contains interstitial granophyric segregations. The clinopyroxene grains are often amphibolized and preserved in relicts. Ilmenite and magnetite form up to 5% of rock volume, and interstitial granophyre composed of quartz, albite, and K-feldspar form several percent of the rock volume.

Fine-grained dolerites occur at ca. 1 m from the dyke contacts. Their main minerals are clinopyroxene (both high-Ca and low-Ca) and plagioclase. The presence of the Fe-rich hornblende, fayalite and quartz-K-feldspar-plagioclase granophyre in the late liquidus assemblage is characteristic for the NW-trending dolerite dykes (Fig. 2b and d). Fayalite constitutes up to 5–7% of the rock volume and crystallized together with opaque minerals, and biotite, hornblende, quartz and granophyre.

The typical accessory minerals of the dolerites are baddeleyite, apatite, chalcopyrite, and rare zircon (Fig. 2d). Sometimes baddeleyite grains are surrounded by a fine zircon rim or contain “ingrowths” of zircon in the central part of grains. Zircon forms small, anhedral metamict grains containing small thorite inclusions. These features of the zircon suggest its xenocrystic origin and indicate crustal contamination of the dolerite parental melts.

Magnetite and ilmenite are typical opaque minerals of the studied dolerites. The Fe-oxide grains usually show a complicated inner structure with V-bearing magnetite grains containing ilmenite exsolution lamella in their cores, and ilmenite in their rims (Fig. 2c). Fe-oxides are often intergrown with fayalite, biotite and amphibole (Fig. 2c).

The central parts of the dykes usually consist of medium-grained clinopyroxene-plagioclase dolerite. These rocks contain up to 5–7% of the granophyre and up to 10% of ilmenite and magnetite. Fayalite is rare or absent. Baddeleyite and rare zircon grains occur in the granophyre intercrystalline space. The amphibole (Cl-bearing

**Table 2**  
U–Pb TIMS isotopic data for baddeleyite from olivine gabbro and dolerite dykes from the Lake Upper Kuito area.

N#	Characteristics: Size ( $\mu\text{m}$ ), number of grains, colour and habit	U/Pb <sup>a</sup>	Pbc/Pbt	$^{206}\text{Pb}/^{204}\text{Pb}^b$	Isotopic ratios corrected for blank and common Pb				Rho	Age (Ma)		
					$^{207}\text{Pb}/^{206}\text{Pb}$	$^{208}\text{Pb}/^{206}\text{Pb}$	$^{207}\text{Pb}/^{235}\text{U}$	$^{206}\text{Pb}/^{238}\text{U}$		$^{207}\text{Pb}/^{235}\text{U}$	$^{206}\text{Pb}/^{238}\text{U}$	$^{207}\text{Pb}/^{206}\text{Pb}$
<b>Ca-230-3</b>												
1	<30, 15, dark-brown, tabular	1.89	0.1	421	0.1570 $\pm$ 1	0.0537 $\pm$ 1	9.7178 $\pm$ 194	0.4488 $\pm$ 11	0.88	2408 $\pm$ 5	2390 $\pm$ 5	2424 $\pm$ 2
2	<30, 10, dark-brown, tabular	2.08	0.02	545	0.1586 $\pm$ 2	0.0347 $\pm$ 2	9.9957 $\pm$ 350	0.4571 $\pm$ 15	0.94	2434 $\pm$ 7	2427 $\pm$ 6	2441 $\pm$ 2
3	<30, 11, dark-brown, tabular	2.10	0.001	967	0.1586 $\pm$ 1	0.0452 $\pm$ 1	10.016 $\pm$ 28	0.4580 $\pm$ 11	0.91	2436 $\pm$ 7	2431 $\pm$ 6	2441 $\pm$ 2
<b>Ca-240-5</b>												
4	50–60, 9, dark-brown, tabular	2.2	0.05	383	0.1468 $\pm$ 2	0.0492 $\pm$ 2	8.5751 $\pm$ 257	0.4237 $\pm$ 12	0.89	2294 $\pm$ 7	2278 $\pm$ 5	2309 $\pm$ 2
5	40–50, 15, pale-brown, long-prism.	2.2	0.04	229	0.1471 $\pm$ 14	0.0713 $\pm$ 4	8.4751 $\pm$ 900	0.4190 $\pm$ 13	0.30	2283 $\pm$ 20	2256 $\pm$ 8	2308 $\pm$ 20
6	40–50, 13, dark-brown, long-prism.	2.9	0.01	406	0.1438 $\pm$ 7	0.0396 $\pm$ 3	6.7373 $\pm$ 404	0.3398 $\pm$ 10	0.48	2078 $\pm$ 12	1886 $\pm$ 6	2274 $\pm$ 10
<b>Ca-245-3</b>												
7	30–40, 14, pale-brown, tabular	2.0	0.08	280	0.1468 $\pm$ 3	0.0465 $\pm$ 2	8.5001 $\pm$ 357	0.4200 $\pm$ 13	0.92	2286 $\pm$ 9	2261 $\pm$ 7	2309 $\pm$ 3
8	<30, 20, pale-brown, long-prism.	2.3	0.01	307	0.1465 $\pm$ 3	0.0343 $\pm$ 3	8.4035 $\pm$ 420	0.4161 $\pm$ 21	0.93	2276 $\pm$ 11	2243 $\pm$ 11	2305 $\pm$ 3
9	<30, 30, dark-brown, long-prism.	2.0	0.09	254	0.1465 $\pm$ 5	0.0582 $\pm$ 3	8.2586 $\pm$ 429	0.4083 $\pm$ 14	0.70	2260 $\pm$ 11	2207 $\pm$ 10	2308 $\pm$ 6
10	<30, 10, pale-brown, long-prism.	1.9	0.25	125	0.1453 $\pm$ 14	0.0707 $\pm$ 4	6.5881 $\pm$ 777	0.3288 $\pm$ 16	0.40	2058 $\pm$ 20	1833 $\pm$ 9	2292 $\pm$ 19

<sup>a</sup> U/Pb ratios for unweighted grains were determined using  $^{202}\text{Pb}/^{235}\text{U}$ ; Pbc, common Pb; Pbt, total Pb.

<sup>b</sup> Measured isotopic ratios; Rho, correlation coefficient of  $^{207}\text{Pb}/^{235}\text{U}$  vs.  $^{206}\text{Pb}/^{238}\text{U}$  ratios; uncertainties ( $2\sigma$ ) refer to last digits of corresponding ratios.



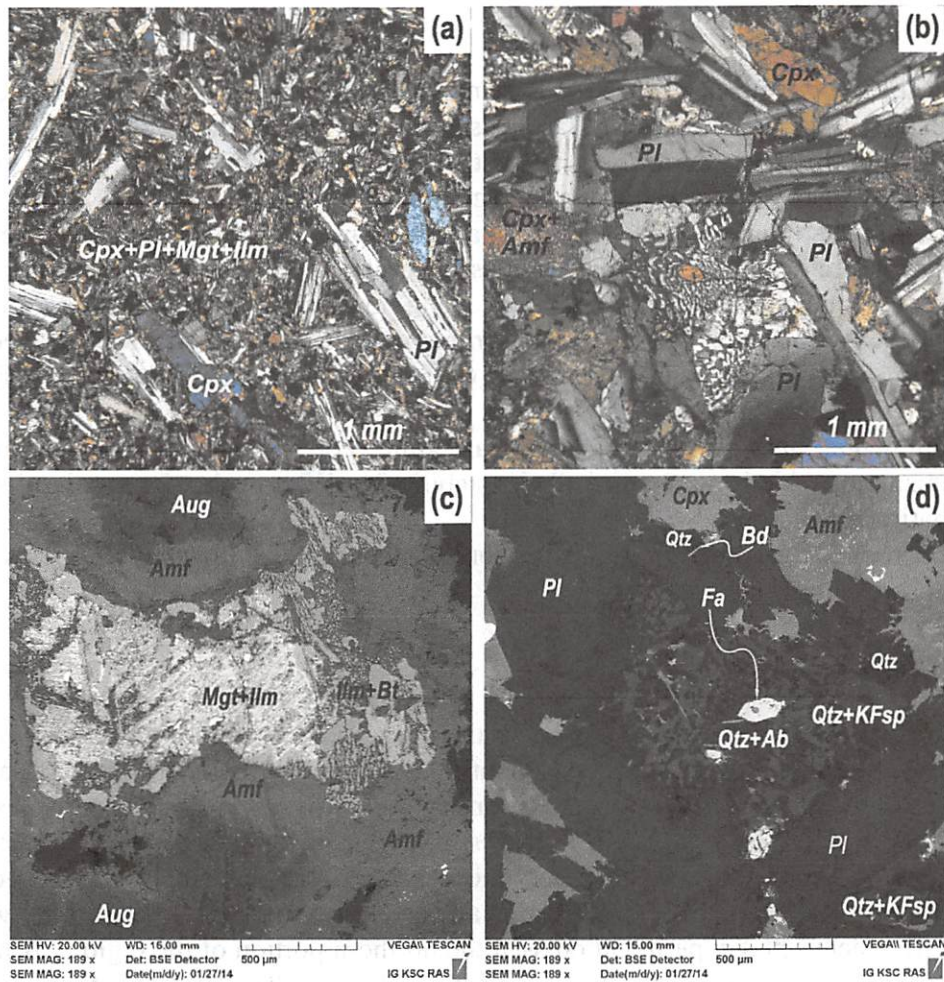


**Fig. 2.** Photomicrographs and back-scattered electron (BSE) images of ca. 2.31 Ga dolerite dykes. Cpx, clinopyroxene; Aug, augite; Pl, plagioclase; Amf, amphibole; Mgt, magnetite; Ilm, ilmenite; Fa, fayalite; Qtz, quartz; KfSp, alkali feldspar; Ab, albite; Bt, biotite; Bd, baddeleyite. (a) Photomicrograph of an Cpx-Pl porphyritic microdolerite, quenched contact rock, sample Ca-240-8, polarized light; (b) photomicrograph of a Fa-bearing dolerite, dyke margin, sample Ca-240-7; (c) Mgt grain with Ilm exsolution lamella surrounded by Ilm + Bt rim, BSE image, sample Ca-245-3; (d) detail of Fig. 2b, BSE image.

Fe-edenite) forms an essential part of the late-magmatic mineral assemblage.

#### 4.3.2. Geochemistry

The fayalite-bearing doleritic dykes of the NW-trending swarm are characterized by a relatively constant chemical composition (Figs. 3–5, Table 1). All dykes have a tholeiitic geochemical affinity. The SiO<sub>2</sub> content varies insignificantly. Low concentrations of MgO and Al<sub>2</sub>O<sub>3</sub> and high concentrations of Fe<sub>2</sub>O<sub>3</sub><sup>tot</sup>, TiO<sub>2</sub>, and P<sub>2</sub>O<sub>5</sub> are characteristic features of these dykes (Fig. 3, Table 1).

Concentrations of the trace-elements in the dykes within the swarm are also nearly-constant. The low content of Cr and Ni corresponds to the low concentrations of MgO in the rocks (Table 1, Fig. 4). At the same time, dolerites have high concentrations of lithophile trace elements (Table 1, Figs. 4 and 5). The distribution of trace elements in dolerites is characterized by enrichment of the LILE and depletion of Nb (Nb/Nb\* = 0.49–0.58) on mantle-normalized diagrams (Fig. 5). Chondrite-normalized REE in the dolerites are relatively flat at the HREE part and display a LREE enrichment ((La/Yb)<sub>n</sub> = 1.50–1.86, (Gd/Yb)<sub>n</sub> = 1.03–1.27) (Fig. 4).

#### 4.3.3. U–Pb study

Baddeleyite from two mafic dykes of the northern (sample Ca-240-5; Fig. 1a and b) and southern (sample Ca-245-3; Fig. 1a and b)

parts of the NW-trending swarm was studied. Sample Ca-240-5 is a coarse-grained dolerite taken from the central part of a ca. 50-m-thick dyke (Fig. 1b). Approximately 100 brownish long-prismatic and dark-brown, tabular baddeleyite grains were extracted from ca. 1.5 kg sample. Three fractions of most transparent, brownish, tabular and long-prismatic grains were analyzed. Each fraction includes 9–15 grains, 40–60 μm in size. Regression of three slightly discordant analyses of baddeleyite (Table 2, lines 4–6) defines an upper intercept age of 2311 ± 5 Ma (MSWD = 0.01) (Fig. 8), interpreted as the emplacement age of the Ca-240 dolerite dyke. The lower intercept age is at 177 ± 110 Ma.

Sample Ca-245-3 is a medium-grained dolerite taken from the central part of the dyke (Fig. 1d). Approximately 250 brownish baddeleyite grains were extracted from ca. 1.5 kg sample. Four fractions of dark brown, tabular and long-prismatic baddeleyite grains were analyzed (Table 2, lines 7–10). Each fraction includes 10–30 grains with crystal size <30 μm to 30–40 μm. Four analyses of baddeleyite define a Discordia with an upper intercept age of 2309 ± 3 Ma (MSWD = 0.84) (Fig. 8), which is interpreted as the dyke emplacement age. The lower intercept age is essentially zero (128 ± 130 Ma).

Taking into account the results of the U–Pb study of baddeleyite from two dykes of similar orientation, their consistent mineral and chemical compositions, the age of the NW-trending swarm is considered to be ca. 2310 Ma.



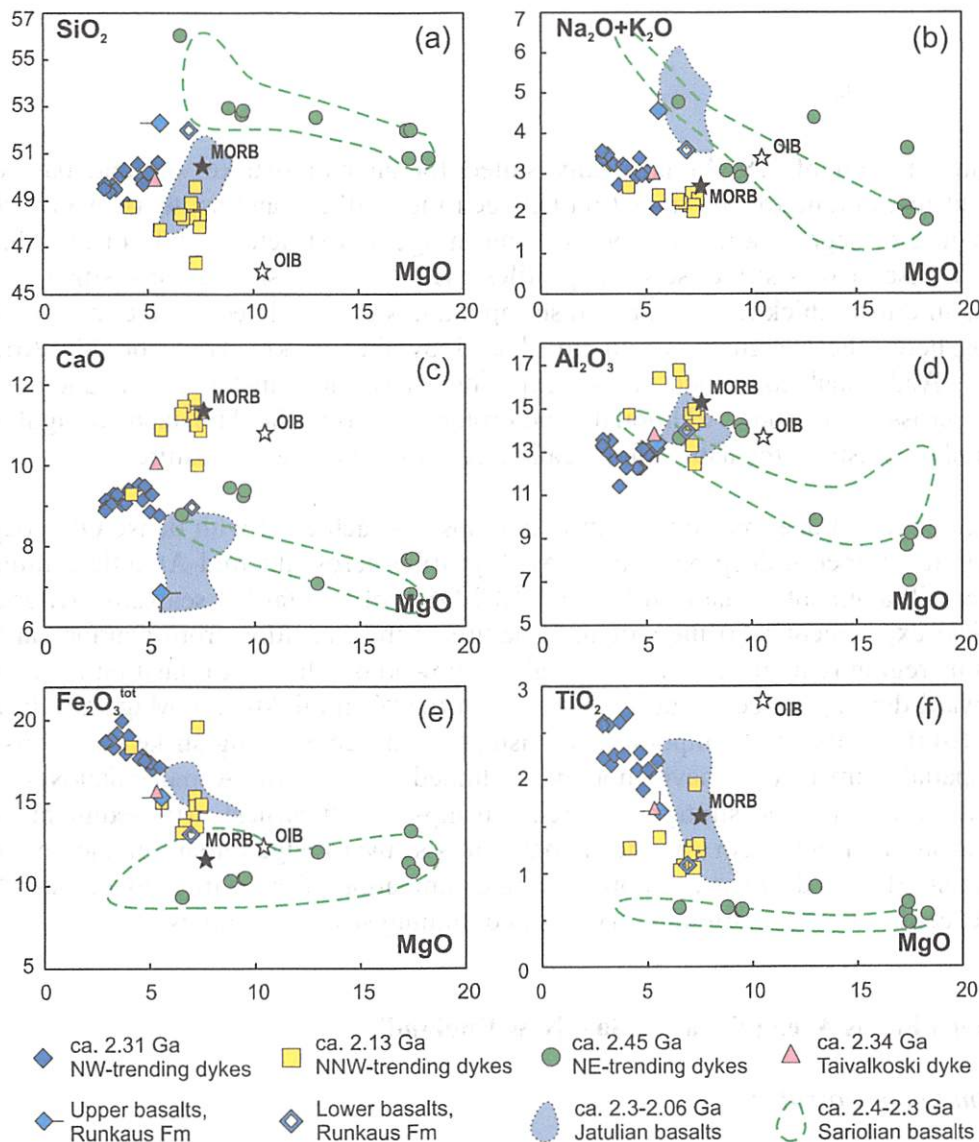


**Fig. 3.** Variations of major elements vs. MgO in Paleoproterozoic mafic dykes and volcanic rocks of the Karelian Craton including ca. 2.31 Ga dolerite dykes; ca. 2.13 Ga continental MORB-type tholeiites dykes (Pirtguba and Allajarvi localities; Stepanova et al., 2014b); ca. 2.45 Ga olivine gabbro-norite dykes of the Lake Upper Kuito area; ca. 2.34 Ga Taivalkoski mafic dyke, (Vuollo and Fedotov, 2005; Salminen et al., 2014); Runkaus metabasalts (Huhma et al., 1990); ca. 2.3–2.06 Ga basalts, Karelian Craton (Malashin et al., 2003); Sariolian mafic volcanic rocks of the Onkamo group (Räsänen et al., 1989).

#### 4.3.4. Sm–Nd study

The Sm–Nd studies were carried out for samples from sites Ca-240 and Ca-245. The results are reported in Table 2. All studied whole-rock samples show uniform initial Nd isotope compositions, with initial  $\epsilon_{Nd}$  values calculated for an emplacement age of 2310 Ma ranging from +0.5 to +0.8.

## 5. Discussion

Three mafic dyke swarm generations were recognized in the Lake Upper Kuito area. They are: (i) ca. 2450 Ma gabbro-norite dykes, (ii) the ca. 2310 Ma dolerite dykes, and (iii) ca. 2130 Ma continental MORB-type tholeiitic dykes.

The NE-trending ca. 2.45 Ga gabbro-norite dykes of the Lashkujarvi swarm correspond to the Sumian (ca. 2.5–2.4 Ga) LIP event that includes high-Mg mafic volcanic rocks, layered intrusions and gabbro-norite dykes (Amelin et al., 1995; Puchtel et al., 1997; Vuollo and Huhma, 2005; Bayanova et al., 2009). Mafic volcanic rocks, mafic

dyke swarms, and layered intrusions of similar age and composition are also recognized in several Precambrian Shields (Bleeker and Ernst, 2006 and references therein). The studied ca. 2450 Ma dykes are typical for the 2.45 Ga event as they have high MgO content, strongly fractionated REE patterns, Nb-depleted primitive mantle-normalized trace-element patterns (Figs. 4 and 5), and negative initial  $\epsilon_{Nd}$  values (Table 1, Fig. 6). Primary melts of ca. 2.45 Ga mafic rocks were produced via high degrees of mantle source melting, and substantial degrees of fractional crystallization and crustal contamination also played an important role in their origin (Puchtel et al., 1997; Hanski et al., 2001b). These mafic rocks are considered to be related to the ascent of a mantle plume (Puchtel et al., 1997; Sharkov et al., 2000; Kulikov et al., 2010).

The NNW-trending ca. 2.13 Ga continental MORB-type tholeiitic dykes correspond to the ca. 2.1 Ga event that also includes mafic volcanic rocks, and Fe–Ti tholeiitic dykes in the Fennoscandian and Canadian Shields (Nykänen et al., 1994; Vuollo and Huhma, 2005; Halls et al., 2008; Maurice et al., 2009; Ernst and Bleeker,



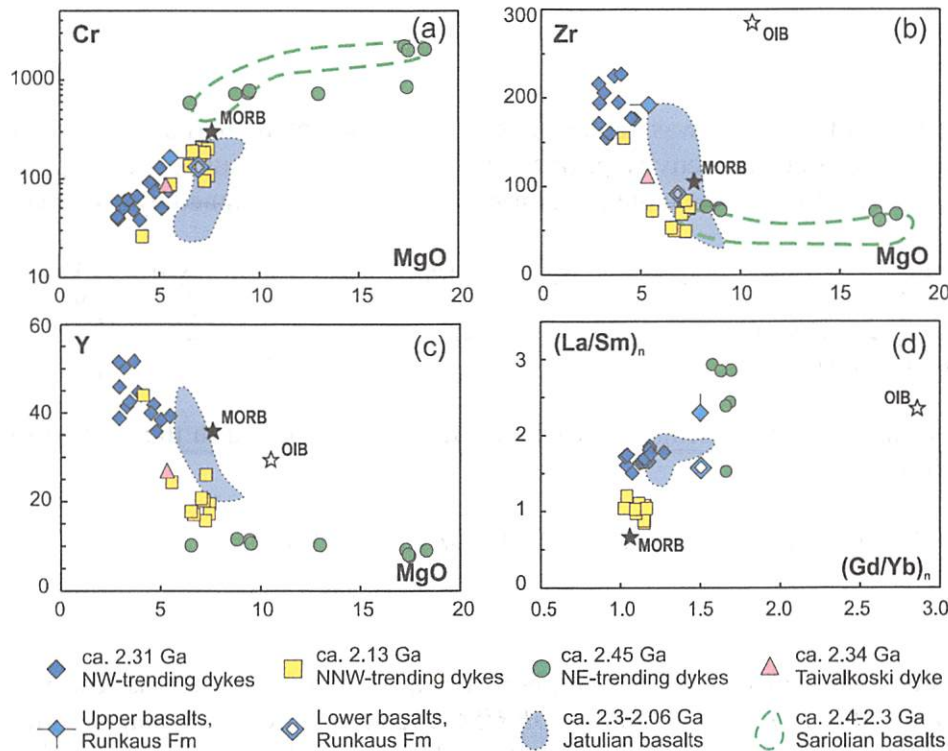


**Fig. 4.** Variations of selected trace elements vs. MgO and  $(La/Sm)_n$  vs.  $(Gd/Yb)_n$  ratios in Paleoproterozoic mafic dykes and volcanic rocks of the Karelian Craton including ca. 2.31 Ga dolerite dykes; ca. 2.13 Ga continental MORB-type tholeiitic dykes (Pirtguba and Allajarvi localities; Stepanova et al., 2014b); ca. 2.45 Ga olivine gabbro dykes of the Lake Upper Kuito area; ca. 2.34 Ga Taivalkoski mafic dyke, (Vuollo and Fedotov, 2005; Salminen et al., 2014); Runkaus metabasalts (Huhma et al., 1990); ca. 2.3–2.06 Ga basalts, Karelian Craton (Malashin et al., 2003); Sariolian mafic volcanic rocks of the Onkamo group (Räsänen et al., 1989).

2010). The ca. 2.13 Ga MORB-type tholeiitic dykes are characterized by low contents of LILE, flat REE patterns, an undepleted HFSE distribution on mantle-normalized diagrams (Fig. 5), and positive initial  $\epsilon_{Nd}$  values varying from +1.4 to +3.0 (Fig. 6). These dykes were described by Stepanova et al. (2014b) and were considered by these authors as indicators of the continental break-up based on the almost uncontaminated character of their melts that formed via DM-type mantle melting at the spinel stability field simultaneously with rapid crustal extension.

In contrast to the ca. 2.45 Ga and ca. 2.1 Ga events that are widespread and relatively well-studied, the 2.31 Ga igneous event falls into the 2.4–2.2 Ga “crustal age gap” period (Condie et al., 2009). Although the amount of data on age of mafic dykes at different Precambrian shields that formed during 2.4–2.2 Ga interval increased dramatically during several past years (French and Heaman, 2010; Nilsson et al., 2012; Partin et al., 2014; Salminen et al., 2014; Davies and Heaman, 2014, this study), the information about petrological process and geodynamic environments during this period for the Fennoscandian (Huhma et al., 1990; Hölttä et al., 2000; Vuollo and Huhma, 2005) and other Precambrian shields (Bleeker and Ernst, 2006; Ernst and Bleeker, 2010) is still limited.

The existence of ca. 2.3 Ga mafic dykes in the Karelian Craton was pointed out by Vuollo and Huhma (2005) who suggested that sporadic dolerite dykes of this age are relatively widespread in the craton. The dolerite dykes with an age  $2339 \pm 18$  Ma occur in the Taivalkoski block in Finland (Salminen et al., 2014). These dykes have an orientation ( $340^\circ$ ) and chemical composition, including the REE and HFSE distribution, similar to those of the studied 2.31 Ga dykes (Figs. 3–5). The Taivalkoski dolerites have a positive initial  $\epsilon_{Nd}$  of +1.4 (Vuollo and Fedotov, 2005) and slightly less evolved chemical composition than that of the studied ca. 2.31 Ga dykes (Figs. 3–5). Taking into account neighbouring position of Voinitsa and Taivalkoski blocks, and similarity in the orientation, mineral

composition, age, and geochemical characteristics of the dykes, the 2.34 Ga Taivalkoski dykes and 2.31 Ga Upper Kuito dykes can be considered as components of a single event. It is also possible that the Runkaus Formation basalts with imprecise Sm–Nd age of  $2330 \pm 180$  Ma (Huhma et al., 1990) that occur in the Peräpohja schist belt between Sariolian conglomerates and Jatulian quartzites form a volcanic counterpart of this event. The basalts of the upper part of the Runkaus Formation have trace-element characteristics (Figs. 3–5), and Nd isotope composition (Fig. 6) close to those of the ca. 2.31 Ga dykes. Thus, it is possible that ca. 2.34 Ga Taivalkoski dykes, 2.31 Ga Lake Upper Kuito dolerite dykes and Runkaus metabasalts belong to a single and relatively widespread endogenic event which we herein term the Kuito–Taivalkoski LIP (cf Taivalkoski LIP name in Ernst, 2014). The origin of these rocks, their tectonic setting, position within regional stratigraphic framework, and relationships with previous and subsequent igneous events have not been discussed previously and are of a considerable interest.

In the regional stratigraphic scale the age of 2.31 Ga corresponds to the boundary between Sariolian (2.4–2.3 Ga) and Jatulian (2.3–2.06 Ga) systems. Despite the fact that formally the 2.31 Ga dykes belongs to the Sariolian sequence they differ from Sariolian volcanic rocks (Figs. 3 and 4) represented by high-Mg, low-Ti tholeiites and vary in composition from komatiites to andesites (Hanski, 2013 and references therein). The initial  $\epsilon_{Nd}$  values of the Sariolian volcanic rocks vary from  $-5.0$  to  $-3.2$  (Hanski, 2013) and differ from those of studied 2.31 Ga dykes. At the same time, the 2.31 Ga dykes have similarity in major and trace-element composition with Jatulian basalts of the Central Karelia (Fig. 5). The observed differences in the contents of CaO, MgO and total alkalis (Fig. 3) could be caused by metasomatic alteration typical for the Jatulian basalts (Ivanikov et al., 2008; Hanski, 2013).

The comparison of ca. 2.31 Ga and ca. 2.45 Ga mafic dyke swarms show considerable differences in age, swarm orientation, mineral



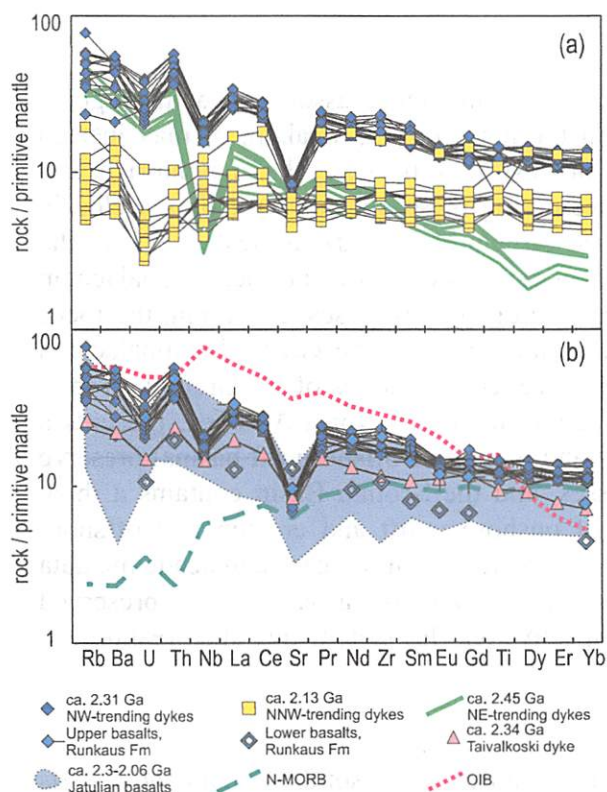


**Fig. 5.** Primitive mantle-normalized patterns for selected trace and rare earth elements for Paleoproterozoic mafic dykes and volcanic rocks of the Karelian Craton including ca. 2.31 Ga dolerite dykes; ca. 2.13 Ga continental MORB-type tholeiitic dykes (Pirtguba and Allajarvi localities; Stepanova et al., 2014b); ca. 2.45 Ga olivine gabbro-norite dykes of the Lake Upper Kuito area; Runkaus metabasalts (Huhma et al., 1990); ca. 2.34 Ga Taivalkoski mafic dyke (Vuollo and Fedotov, 2005; Salminen et al., 2014); ca. 2.3–2.06 Ga basalts, Karelian Craton (Malashin et al., 2003); N-MORB average composition (Hofmann, 1988); OIB average composition (Sun and McDonough, 1989). Normalization values from McDonough and Sun (1995).

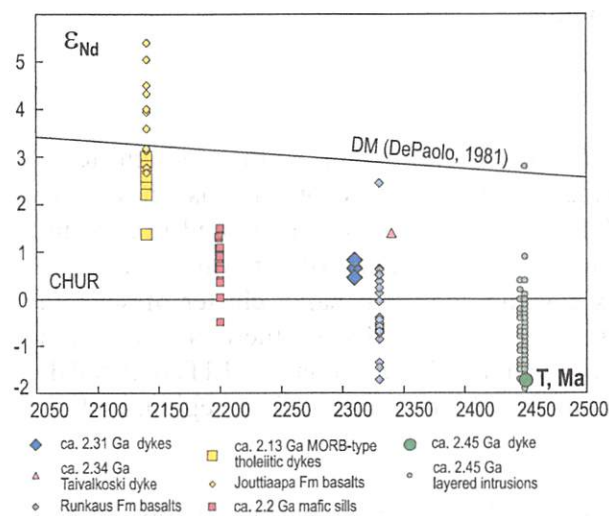


**Fig. 6.** Diagram of initial  $\epsilon_{Nd}$  values vs. age for Paleoproterozoic mafic igneous rocks of the Karelian Craton including ca. 2.31 Ga dolerite dykes; ca. 2.34 Ga Taivalkoski dyke (Salminen et al., 2014; Vuollo and Fedotov, 2005); Runkaus and Jouttiaapa Formations volcanic rocks, Peräpohja schist belt (Huhma et al., 1990); ca. 2.13 Ga continental MORB-type tholeiitic dykes (Stepanova et al., 2014b); ca. 2.2 Ga mafic sills (Hanski et al., 2010); ca. 2.45 Ga olivine gabbro-norite dyke, and ca. 2.45 Ga layered intrusions (Amelin and Semenov, 1996).

composition, major-element concentrations, trace-element distribution and Nd isotope composition (Figs. 3–6, Table 1) These distinctions suggest contrastingly different petrological and tectonic processes responsible for the origin of the ca. 2.45 Ga and 2.31 Ga dyke swarms.

The ca. 2.31 Ga dykes also differ from ca. 2.13 Ga swarm recognized in the studied area. The clinopyroxene–plagioclase porphyrites are characteristic for the 2.31 Ga dolerites in contrast to the ca. 2.13 Ga continental MORB-type tholeiitic dykes that are mostly aphyric. Clinopyroxene and plagioclase are the main minerals in both cases, but in the continental MORB-type tholeiites they are more primitive. These rocks are also different in terms of the composition of the late magmatic mineral assemblage. In the continental MORB-type tholeiites, it includes Cl-bearing edenite, plagioclase ( $An_{25}$ ), and quartz, but Fa-bearing quartz–K-feldspar–albite–apatite granophyre is typical of the ca. 2.31 Ga dolerite dykes (Figs. 2b, 2d). The 2.31 Ga dolerites have essentially lower contents of MgO, Cr, Ni, and higher concentrations of  $TiO_2$ ,  $Fe_2O_3^{tot}$  and most part of lithophile trace elements than MORB-type tholeiites (Figs. 3 and 4). They are also more enriched in LREE, LILE and depleted in Nb compared to MORB-type tholeiites (Fig. 5).

It should be noted that despite the differences indicated above, ca. 2.31 Ga dykes and ca. 2.13 Ga continental MORB-type tholeiitic dykes show certain similarities in the distribution of major and trace elements (Figs. 3–5). Chemical composition the ca. 2.31 Ga dolerites close to those of gabbro–pegmatites of the MORB-type tholeiitic dykes (Figs. 3–5) corresponding to the late residual melts formed by in situ fractional crystallization (Stepanova et al., 2014b). Both the ca. 2.31 Ga and 2.13 Ga dykes have flat or near-flat HREE distribution patterns (Fig. 5). Geochemical characteristics of the ca. 2.31 Ga and 2.13 Ga dykes allow us to propose similar origin of their primary mantle melts but different history of crustal evolution. To test this hypothesis, we consider petrological processes that could be responsible for the evolution of primary melts of ca. 2.31 Ga dykes.

## 5.1. Petrology of the 2.31 Ga dykes

### 5.1.1. Fractional crystallization

Very low contents of MgO, Cr, Ni, and high contents of  $Fe_2O_3^{tot}$  and  $TiO_2$  in the ca. 2.31 Ga dolerites are indicative of the evolved character of their magmas that could be considered as a result of a significant role of fractional crystallization in their parental magmas evolution. There are no signs of in situ fractional crystallization such as layering or gabbro–pegmatite schlieren in the studied dykes. All of them consist of massive dolerites whose chemical and mineral compositions vary insignificantly across the dyke. However, in situ crystallization processes are well-defined microscopically.

Based on the composition of the main minerals, in situ crystallization processes in the dykes could be subdivided into two main stages. The first one includes crystallization of relatively high-Mg augite, pigeonite ( $X_{Mg} = 0.5–0.6$ ), plagioclase ( $An_{60–45}$ ), and probably magnetite that form the “framework” of the rock. The second stage comprises crystallization of the residual liquids enriched in  $SiO_2$ ,  $Fe_2O_3^{tot}$ ,  $TiO_2$ , incompatible trace elements, and depleted in MgO and CaO, resulting in mineral assemblages that include high-Fe clinopyroxene, Fe–edenite, plagioclase ( $An_{25}$ ), ilmenite, and then fayalite, quartz, K-feldspar, albite, and apatite. The enrichment of the system in  $SiO_2$  and very low  $fO_2$  values ( $-2QFM$  or  $-3QFM$  based on modelling results and measured  $FeO/Fe_2O_3$  ratios in the rocks; Stepanova, 2004) probably caused the crystallization of fayalite from the residual melts.

An attempt to evaluate the PT-parameters of crystallization using clinopyroxene thermobarometers of Putirka (2008) has not been successful because clinopyroxene was not in equilibrium



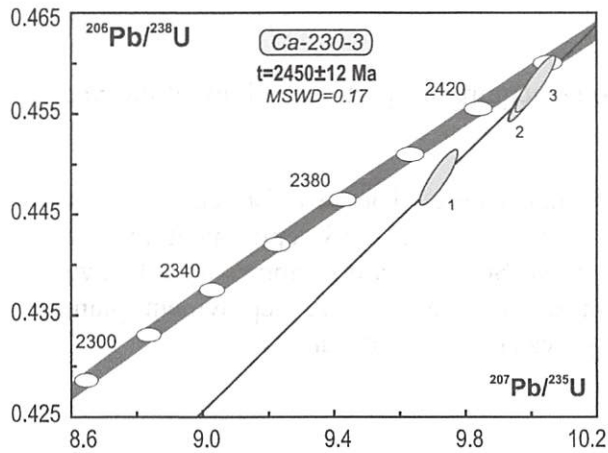


Fig. 7. U–Pb concordia diagram showing baddeleyite analyses and calculated discordia line. Sample Ca-230-3.

with the melt corresponding to the whole-rock composition, but likely crystallized at depth in an intermediate magma chamber. The clinopyroxene barometer of Nimis (1995) gives an estimate for the crystallization pressure at ca. 1 kbar or less, which is consistent with early crystallization of the plagioclase phenocrysts in the rocks.

The composition of the dolerites suggests early crystallization of a gabbroic mineral assemblage in the intermediate magma chamber and probably olivine removal from the system at early stages of a primitive melt crystallization that caused the strong depletion of the rocks in Mg and Ni. Very high contents of the  $\text{Fe}_2\text{O}_3^{\text{tot}}$  in the dolerites suggest low  $f\text{O}_2$  at early stages of the parental melts evolution and a Fenner-type (Fenner, 1929) crystallization path. Taking into account these boundary conditions reverse fractional crystallization modelling was carried out using the Petrolog 3.0 software (Danyushevsky and Plechov, 2011) at  $P=3$  kbar and  $f\text{O}_2=\text{QFM}$  (Table 1). The result of calculations indicates that addition of 45–50% of olivine–plagioclase–clinopyroxene cumulate to the relatively primitive dolerite composition corresponding to the sample Ca-246-1 could give the melts similar to average N-MORB (Hofmann, 1988).

### 5.1.2. Crustal contamination

Several features of the studied ca. 2.31 Ga dykes are indicative of crustal contamination. The dykes contain a large amount of quartz–feldspar-bearing granophyric material that sometimes contains zircon xenocrysts even in the chilled margin zones. The geochemical signatures of the 2.31 Ga doleritic dykes, such as enrichment

in LIL elements and depletion of Nb on mantle-normalized multi-element diagrams (Fig. 5), and the low positive initial  $\epsilon_{\text{Nd}}$  values from +0.5 to +0.8 also provide strong evidence for crustal contamination processes. A rough estimate of the degree of crustal contamination and contaminant composition was obtained by binary mixing calculation. Several potential contaminants typical for the continental crust of the Western Karelian terrane of the Karelian Craton were considered. They are ca. 2.8 Ga TTG gneisses, ca. 2.74 Ga granulites of Voknavolok block, and ca. 2.71 Ga sanukitoid series granodiorites (Lobach-Zhuchenko et al., 2000; Samsonov et al., 2001; Bibikova et al., 2005). An average composition of N-MORB (DePaolo, 1981; Hofmann, 1988) recalculated to 2.31 Ga was considered the primitive uncontaminated melt end-member. The results of the calculation indicate that the most probable contaminant corresponds to the sanukitoid series granodiorite and its contribution to the melt could be evaluated at 12–14% (Fig. 9). According to the calculation, the ca. 2.8 Ga TTG gneisses is another likely contaminant. In this case, the degree of crustal contamination reached about 25% (Fig. 9), but so high degree of contamination is contrary with relatively low  $\text{SiO}_2$  contents in studied dolerites. The Voknavolok granulites turned out to be unlikely contaminant.

### 5.1.3. Mantle melting

Due to the evolved geochemical composition of the ca. 2.31 Ga mafic dykes, neither the degree of mantle melting nor the composition of primary melts could not be precisely evaluated. Nevertheless, two parameters can be discussed. The near-chondritic HREE ratios ( $(\text{Gd}/\text{Yb})_n = 1.03\text{--}1.27$ ) of the dolerites suggest that the primary melts of ca. 2.31 Ga dolerites were not in equilibrium with garnet and formed at a relatively shallow level of the mantle in the spinel peridotite stability field. The initial  $\epsilon_{\text{Nd}}$  values of the dolerites those vary from +0.5 to +0.8 together with evidences for crustal contamination suggest that their primary melts were originated by partial melting of a long-term depleted mantle source and subsequent assimilation and fractional crystallization processes.

### 5.2. Tectonic position and relation to continental break-up events

The compositional and petrological differences between studied intraplate mafic igneous events of age ca. 2.45, 2.31 and 2.13 Ga in the Karelian Craton are probably resulting from their different tectonic setting. The well-studied 2.45 Ga high-Mg tholeiites are usually considered to be related to the ascent of a high-temperature mantle plume which most likely did not lead to a break-up of the Archaean continental lithosphere of the Karelian Craton (Puchtel et al., 1997; Sharkov et al., 2000; Kulikov et al., 2010). The ca. 2.13 Ga continental MORB-type tholeiitic dykes considered as

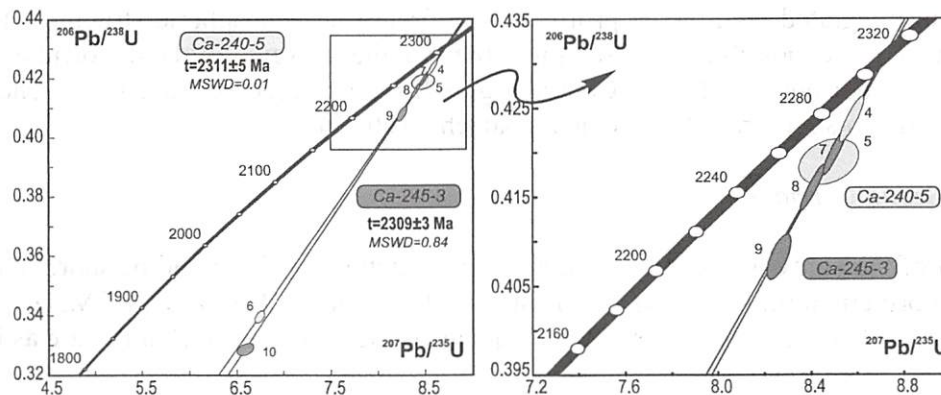
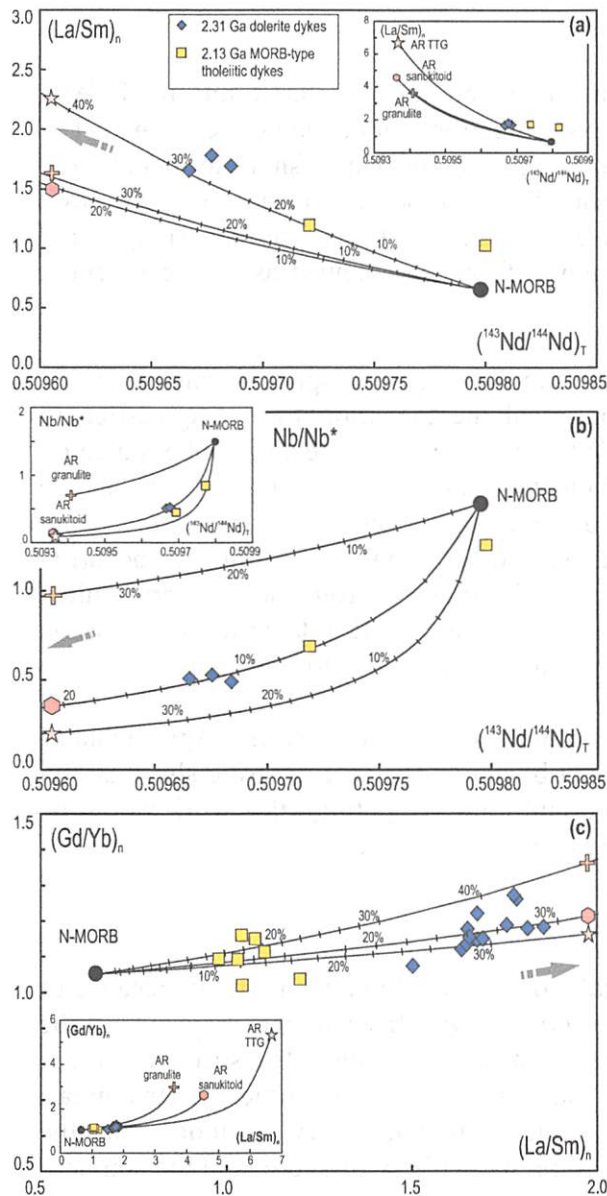


Fig. 8. U–Pb concordia diagram showing baddeleyite analyses and calculated discordia lines. Samples Ca-240-5, Ca-245-3.





**Fig. 9.** Selected trace element ratios and Nd isotope composition illustrating the effects of crustal contamination (via bulk mixing) on magmas derived from an average N-MORB (Hofmann, 1988) via assimilation of Archaean sanukitoid, adakite series TTG gneiss and Voknavolok complex granulite contaminant. The compositions of the contaminant endmembers are compiled from the data of Bibikova et al. (2005), Lobach-Zhuchenko et al. (2000), and Samsonov et al. (2001).

probable indicators of a continental break-up (Stepanova et al., 2014b). Newly identified ca. 2.31 Ga dolerite dykes are clearly different from the ca. 2.45 Ga high-Mg tholeiites, but similar with 2.13 Ga continental MORB-type tholeiitic dykes. It probably suggests the similarity in tectonic setting for the 2.31 Ga and 2.13 Ga dykes. Indeed, the fact that studied ca. 2.31 Ga dykes form a relatively wide, regular swarm consisting of ca. 50 m thick dykes indicates that it formed due to intensive extension over a relatively large segment of the Archaean continental crust. The dolerites are highly contaminated and have undergone a substantial degree of fractional crystallization, which suggests a long-term storage in an intracrustal magma chamber and a relatively slow ascent of the melts to the surface. This is contrary with rapid crustal extension, lithospheric rapture and continental break-up at ca. 2.31 Ga, but rather indicates the existence of a relatively stable extensional

tectonic environment that could be regarded as an unsuccessful break-up attempt. Taking into account that Karelian Craton is considered to be a part of a proposed supercontinent Superia (e.g. Bleeker and Ernst, 2006; Söderlund et al., 2010) it could be suggested that this supercontinent or at least a large block of the Archaean continental lithosphere corresponding to the Fennoscandia remained relatively stable at ca. 2.31–2.34 Ga. It was broken-up substantially later probably at ca. 2.1 Ga. To test this hypothesis further geochronological and paleomagnetic investigations are required.

The ca. 2.31 Ga event is relatively voluminous and could be considered as a fragment of relatively large igneous event, e.g. large igneous province (LIP, e.g. Ernst, 2014), thus it should be assumed that the number and intensity of endogenous events of age 2.4–2.2 Ga are greatly undervalued and need further study. This also strongly argues against a decrease of endogenic activity and magmatic “slowdown” during ca. 2.4–2.2 Ga period.

Several important issues related to the origin of the ca. 2.31 Ga event remain unresolved. What caused the mantle melting? This question is especially important given the fact that information on mantle melting events of this age is very restricted. Part of the available data, such as the rock compositions similar to ca. 2.3–2.06 Ga continental flood basalts and the occurrence of the near-contemporaneous quartzite cover, could be considered within the model of a mantle plume ascent, plume-related mantle melting, and near-simultaneously areal uplift. Such interpretation contradicts the absence of high-Mg rocks among the studied 2.31 Ga dykes that could be formed via high-degree, deep-seated mantle melting. Another possible scenario for the mantle melting could be the delamination of eclogitized lower crust that formed due to mafic magma underplating in the previous, ca. 2.45 Ga igneous event. To choose between these two models, the additional data on the ca. 2.3 Ga mafic dykes and basalts are required. The search for the relatively primitive mafic rocks of the same age that could give more reliable information on the mantle melting processes and primary melts evolution is an important objective of further studies.

## 6. Conclusions

Three mafic dyke generations were recognized in the Lake Upper Kuito area in the Western Karelian terrane of the Karelian Craton. They are: (i) ca. 2450 Ma gabbronorite dykes of Lashkujarvi swarm, (ii) the ca. 2310 Ma dolerite dykes of Kuito swarm, and (iii) ca. 2130 Ma continental MORB-type tholeiitic dykes of Pirtguba swarm. Each swarm is related to a distinct intraplate igneous event, which indicates that specific mantle melting processes and extensional processes caused injection of melts into upper levels of the continental crust.

Geochemical characteristics of the 2.31 Ga dolerite dykes in the Lake Upper Kuito area are close to those of the ca. 2.3 Ga Runkaus Formation basalts from Peräpohja schist belt (Huhma et al., 1990) and the ca. 2.34 Ga mafic dykes in the Taivalkoski block (Salminen et al., 2014). It suggests that they could belong to a single igneous event spread in a relatively wide area. It gives new evidence for an intensive magmatic activity at ca. 2.3 Ga that contradicts with the idea of decreasing of endogenic activity and magmatic “slowdown” during ca. 2.4–2.2 Ga period (Condie et al., 2009).

The geochemical and isotopic characteristics of the ca. 2.31 Ga dolerites, and modelling results allow us to suggest that (1) high concentrations of the lithophile elements in the dolerites resulted from high degrees of fractional crystallization, and not from the source enrichment; (2) the degree of crustal contamination is estimated at 12–14%; (3) a melt which is similar in chemical composition to the studied dolerites could be generated via 45–50% fractional crystallization of the N-MORB composition at the QFM



fO<sub>2</sub> level; (4) the primary melts could be a result of melting of a DM-type mantle in the spinel peridotite stability field.

Geochemical characteristics of the ca. 2.31 Ga dolerite dykes are clearly different from those of the ca. 2.45 Ga gabbroites but the former show a considerable similarity to ca. 2.13 Ga continental MORB-type tholeiites, which could be caused by similar tectonic and mantle dynamic processes operating in the ca. 2.13 and ca. 2.31 events. The main difference between these two events is a long-lasting storage of the mantle melts in the continental crust and a relatively low speed of their ascent to the surface at ca. 2.31 Ga.

These features indicate that ca. 2.31 Ga event was not related to a break-up of the continental lithosphere of the Karelian Craton, but can be regarded as an unsuccessful break-up attempt or a pre-breakup event.

## Acknowledgments

Alexandra Stepanova is grateful to Ulf Söderlund for his advice on baddeleyite extraction and the opportunity to work in the Mineral separation Laboratory at the University of Lund. Svetlana Bogdanova and Alexander Kotov are gratefully thanked for their general support at the early stages of this study. The suggestive and constructive reviews of Richard Ernst and two anonymous reviewers that significantly improved the manuscript are greatly appreciated. The editorial handling by Sergei Pisarevsky is gratefully acknowledged.

The reported study was partially supported by RFBR, research project 14-05-00432.

## References

- Amelin, Y.V., Semenov, V.S., 1996. Nd and Sr isotopic geochemistry of mafic layered intrusions in the eastern Baltic shield: implications for the evolution of Paleoproterozoic continental mafic magmas. *Contrib. Mineral. Petrol.* 124, 255–272.
- Amelin, Y.V., Heaman, L.M., Semenov, V.S., 1995. U–Pb geochronology of layered mafic intrusions in the eastern Baltic Shield: implications for the timing and duration of Paleoproterozoic continental rifting. *Precambrian Res.* 75, 31–46.
- Aspler, L.B., Cousens, B.L., Chiarenzelli, J.R., 2002. Griffin gabbro sills (2.11 Ga), Hurwitz Basin, Nunavut, Canada: long-distance lateral transport of magmas in western Churchill Province crust. *Precambrian Res.* 117, 269–294.
- Bayanova, T., Ludden, J., Mitrofanov, F.P., 2009. Timing and duration of Paleoproterozoic events producing ore-bearing layered intrusions of the Baltic Shield: metallogenic, petrological and geodynamic implications. *Geol. Soc. Lond. (Special Publications)* 323, 165–198.
- Bibikova, E.V., Samsonov, A.V., Petrova, A.Y., Kirnozova, T.I., 2005. The Archean geochronology of Western Karelia. *Stratigr. Geol. Correl.* 13, 459–475.
- Bleeker, W., Ernst, R., 2006. Short-lived mantle generated magmatic events and their dyke swarms: the key unlocking Earth's paleogeographic record back to 2.6 Ga. In: Hanski, E., Mertanen, S., Rämö, T., Vuollo, J. (Eds.), *Dyke Swarms – Time Markers of Crustal Evolution*. Taylor & Francis Group, London, pp. 3–26.
- Buiko, A., Levchenkov, O., Turchenko, S., Drubetskoi, E., 1995. Geology and isotopic dating of the early Proterozoic Sumian-Sariolian Complex in northern Karelia (Paanajärvi-Tsipringa structure). *Stratigr. Geol. Correl.* 3, 16–30.
- Condie, K.C., O'Neill, C., Aster, R.C., 2009. Evidence and implications for a widespread magmatic shutdown for 250 My on Earth. *Earth Planet. Sci. Lett.* 282, 294–298.
- Corfu, F., Bayanova, T.B., Shchiptsov, V.V., Frantz, N., 2011. U–Pb ID-TIMS age of the Tikshezero carbonatite: expression of 2.0 Ga alkaline magmatism in Karelia, Russia. *Cent. Eur. J. Geosci.* 3, 302–308.
- Danyushevsky, L., Plechov, P., 2011. Petrolog3: integrated software for modeling crystallization processes. *Geochem. Geophys. Geosyst.* 12 (7), Q07021, <http://dx.doi.org/10.1029/2011GC003516>.
- Davies, J.H.F.L., Heaman, L.M., 2014. New U–Pb baddeleyite and zircon ages for the Scourie dyke swarm: a long-lived large igneous province with implications for the Paleoproterozoic evolution of NW Scotland. *Precambrian Res.* 249, 180–198.
- Ein, A.S., 1984. Mafic dikes of northern Karelia. In: Bogachev, A.I., Stepanov, V.S., Lavrov, M.M., Sluysarev, V.D., Gorbik, N.A. (Eds.), *Intrusive Basites and Hyperbasites of Karelia*. Petrozavodsk, pp. 30–41 (in Russian).
- Eriksson, P.G., Condie, K.C., 2014. Crustal sedimentation regimes in the ca. 2450–2000 Ma period: relationship to a possible widespread magmatic slowdown on Earth? *Gondwana Res.* 25, 30–47.
- Ernst, R.E., 2014. *Large Igneous Provinces*. Cambridge University Press, pp. 653.
- Ernst, R.E., Bleeker, W., 2010. Large igneous provinces (LIPs), giant dyke swarms, and mantle plumes: significance for breakup events within Canada and adjacent regions from 2.5 Ga to the present. *Can. J. Earth Sci.* 47, 695–739.
- Ernst, R.E., Buchan, K.L., 2001. The use of mafic dike swarms in identifying and locating mantle plumes. *Geol. Soc. Am. (Special Papers)* 352, 247–265.
- Fenner, C.N., 1929. The crystallization of basalts. *Am. J. Sci.* 105, 225–253.
- French, J.E., Heaman, L.M., 2010. Precise U–Pb dating of Paleoproterozoic mafic dyke swarms of the Dharwar Craton, India: implications for the existence of the Neoproterozoic supercraton Scavia. *Precambrian Res.* 183, 416–441.
- Glushanin, L.V., Sharov, N.V., Shchiptsov, V.V., 2011. (Onezhskaya Paleoproterozoic structure (geology, tectonics, deep structure and metallogeny)). KRC RAS, Petrozavodsk (in Russian).
- Halls, H.C., Davis, D.W., Stott, G.M., Ernst, R., Hamilton, M.A., 2008. The Paleoproterozoic Marathon Large Igneous Province: new evidence for a 2.1 Ga long-lived mantle plume event along the southern margin of the North American Superior Province. *Precambrian Res.* 162, 327–353.
- Hanski, E., 2013. Evolution of the Paleoproterozoic (2.50–1.95 Ga) non-orogenic magmatism in the eastern part of the Fennoscandian Shield. In: Melezhik, V.A., Prave, A.R., Fallick, A.E., Kump, L.R., Strauss, H., Lepland, A., Hanski, E.J. (Eds.), *Reading the Archive of Earth's Oxygenation, Volume 1: The Paleoproterozoic of Fennoscandia as Context for the Fennoscandian Arctic Russia – Drilling Early Earth Project*. Springer-Verlag, Berlin, Heidelberg, pp. 179–245.
- Hanski, E., Huhma, H., Vuollo, J., 2010. SIMS zircon ages and Nd isotope systematics of the 2.2 Ga mafic intrusions in northern and eastern Finland. *Bull. Geol. Soc. Finl.* 82, 31–62.
- Hanski, E.J., Melezhik, V.A., 2013. Litho- and chronostratigraphy of the Paleoproterozoic Karelian formations. In: Melezhik, V.A., Prave, A.R., Fallick, A.E., Kump, L.R., Strauss, H., Lepland, A., Hanski, E.J. (Eds.), *Reading the Archive of Earth's Oxygenation, Volume 1: The Paleoproterozoic of Fennoscandia as Context for the Fennoscandian Arctic Russia – Drilling Early Earth Project*. Springer-Verlag, Berlin, Heidelberg, pp. 39–110.
- Hanski, E., Huhma, H., Rastas, P., Kamenetsky, V.S., 2001a. The Paleoproterozoic komatiite-picrite association of Finnish Lapland. *J. Petrol.* 42, 855–876.
- Hanski, E., Walker, R.J., Huhma, H., Suominen, I., 2001b. The Os and Nd isotopic systematics of the 2.44 Ga Akanvaara and Koitelainen mafic layered intrusions in northern Finland. *Precambrian Res.* 109, 73–102.
- Heilimo, E., Halla, J., Huhma, H., 2011. Single-grain zircon U–Pb age constraints of the western and eastern sanukitoid zones in the Finnish part of the Karelian Province. *Lithos* 121, 87–99.
- Hofmann, A.W., 1988. Chemical differentiation of the Earth: the relationship between mantle, continental crust, and oceanic crust. *Earth Planet. Sci. Lett.* 90, 297–314.
- Hölttä, P., Huhma, H., Mänttari, I., Paavola, J., 2000. P–T–t development of Archean granulites in Varpaisjärvi, Central Finland II. Dating of high-grade metamorphism with the U–Pb and Sm–Nd methods. *Lithos* 50, 97–120.
- Hölttä, P., Balagansky, V., Garde, A.A., Mertanen, S., Peltonen, P., Slabunov, A., Sorjonen-Ward, P., Whitehouse, M., 2008. Archean of Greenland and Fennoscandia. *Episodes* 1, 13–19.
- Huhma, H., Cliff, R.A., Perttunen, V., Sakko, M., 1990. Sm–Nd and Pb isotopic study of mafic rocks associated with early Proterozoic continental rifting: the Peripohja schist belt in northern Finland. *Contrib. Mineral. Petrol.* 104, 369–379.
- Ilijina, M., Hanski, E., 2005. Layered mafic intrusions of the Tornio-Näränkävaara belt. In: Lehtinen, M., Nurmi, P.A., Rämö, O.T. (Eds.), *Precambrian Geology of Finland – Key to the Evolution of the Fennoscandian Shield*. Elsevier, Amsterdam, pp. 101–137.
- Ivanikov, V.V., Malashin, M.V., Golubev, A.I., Philippov, N.B., 2008. New data on the geochemistry of the Jatulian basalts, Central Karelia. *St.-Petersb. State Univ. Bull. Ser. Geol. Geogr.* 4, 30–44.
- Karandashev, V.K., Turanov, A.N., Orlova, T.A., Lezhnev, A.E., Nosenko, S.V., Zolotareva, N.I., Moskvitina, I.R., 2008. Use of the inductively coupled plasma mass spectrometry for element analysis of environmental objects. *Inorg. Mater.* 44, 1491–1500.
- Kontinen, A., Paavola, J., Lukkarinen, H., 1982. K–Ar ages of hornblende and biotite from Late Archean rocks of eastern Finland – interpretation and discussion of tectonic implications. *Geol. Surv. Finl. Bull.* 365, 31.
- Korsakova, M.A., Myskova, T.A., Ivanov, N.M., 2011. Granitoids of Sumian age in the south-east part of the North-Karelian zone. *Geol. Miner. Resour. Karel.* 14, 57–71 (in Russian).
- Kovalenko, A., Clemens, J.D., Savatenkov, V., 2005. Petrogenetic constraints for the genesis of Archean sanukitoid suites: geochemistry and isotopic evidence from Karelia, Baltic Shield. *Lithos* 79, 147–160.
- Kozhevnikov, V.N., 1982. Origin of the Structural-Metamorphic Paragenesis in the Precambrian Complexes. *Nauka, Leningrad* (in Russian).
- Kulikov, V.S., Bychkova, Y.V., Kulikova, V.V., Ernst, R.E., 2010. The Vetryny Poyas (Windy Belt) subprovince of southeastern Fennoscandia: an essential component of the ca. 2.5–2.4 Ga Sumian large igneous provinces. *Precambrian Res.* 183, 589–601.
- Kusky, T.M., Li, J., 2003. Paleoproterozoic tectonic evolution of the North China Craton. *J. Asian Earth Sci.* 22, 383–397.
- Lauri, L.S., Mikkola, P., Karinen, T., 2012. Early Paleoproterozoic felsic and mafic magmatism in the Karelian province of the Fennoscandian shield. *Lithos* 151, 74–82.
- Larionova, Y.O., Samsonov, A.V., Shatagin, K.N., 2007. Sources of Archean sanukitoids (high-Mg subalkaline granitoids) in the Karelian craton: Sm–Nd and Rb–Sr isotopic-geochemical evidence. *Petrology* 15, 530–550.
- Larionova, Y.O., Samsonov, A.V., Shatagin, K.N., Nosova, A.A., 2013. Isotopic geochemical evidence for the Paleoproterozoic age of gold mineralization in Archean greenstone belts of Karelia, the Baltic Shield. *Geol. Ore Depos.* 55, 320–340.